 doi:10.20944/preprints202008.0576.v1

The description of heat capacity by the Debye – Mayer – Kelly hybrid model

Valery P. Vassiliev [1)], Alex F. Taldrik [2)]

[1)] *Lomonosov Moscow State University, Chemistry Department, 119991 Moscow, Russia* valeryvassiliev@yahoo.fr *(*)*

[2)] *Institute of Superconductivity and Solid State Physics; 1, Kurchatov Sq., 123182 Moscow, Russia* taldrik48@yandex.ru

Abstract

The universal Debye – Mayer – Kelly hybrid model was proposed for the description of the heat capacity from 0 K to the melting points of substance within the experimental uncertainty for the first time. To describe the heat capacity, the in-house software on the base of commercial one DELPHI-7 was used with a 95% confidence level. To demonstrate the perfect suitability of this model, a thermodynamic analysis of the heat capacities of the fourth group elements, and some compounds of the $A^{III}B^{V}$ and $A^{II}B^{VI}$ phases was carried out. It produced good agreement within the experimental uncertainty. There is no a similar model description in literature.

The Similarity Method is a convenient and effective tool for critical analysis of the heat capacities of isostructural phases, which was used as an example for diamond-like compounds. Phases with the same sum of the atomic numbers of elements (Z), such as diamond and $B_{0.5}N_{0.5\,(cub)}$ (Z = 6); pure silicon (Si) and $Al_{0.5}P_{0.5}$ (Z=14); pure germanium (Ge) and $Ga_{0.5}As_{0.5}$ (Z = 32)); pure grey tin (alpha-Sn) and $In_{0.5}Sb_{0.5}$, and $Cd_{0.5}Te_{0.5}$ (Z = 50) have the same heat capacity experimental values in the solid state. The proposed

 doi:10.20944/preprints202008.0576.v1

models can be used to both different binary and multicomponent phases. It helps to standardize the physicochemical constants.

Key words: Heat Capacity; Entropy; Similarity Method; $A^{III}B^{V}$, $A^{II}B^{VI}$ Phases; Pure Elements IV Group

1. Introduction

Despite the fact that significant experimental data on various physicochemical constants have been accumulated to date, the problem of standardizing these constants has arisen because mathematical modeling only exacerbates this problem. The concept of the relation of physicochemical constants of isostructural compounds with the Periodic Law is taken as a basis for this discussion.

Our previous review articles [1] evidenced the relation of thermodynamic data with Periodic Law and established a strict relationship between the enthalpy of formation, melting point and the atomic numbers of components in the semiconductor $A^{III}B^{V}$ phases, with the diamond-like structure of sphalerite and wurtzite types.

The proposed model was used for the critical assessment of the thermodynamic properties of isostructural compounds. The relationship between the reduced enthalpy, standard entropy, reduced Gibbs energy and the sum of the atomic numbers ($Z_i = Z_A + Z_B$) has been used for the critical assessment of the thermodynamic properties of $A^{III}B^{V}$ phases. In this work, the Similarity Method was applied to the critical analysis of heat capacities in the solid state of the diamond-like phases. The relationship of the heat capacities of $A^{III}B^{V}$ phases vs. the logarithm of the sum of atomic numbers of elements of the $A^{III}B^{V}$ phases (sphalerite and wurtzite types) were used to estimate the continuum above 298 K [2]. In the present work, the Debye – Mayer – Kelly hybrid model was proposed for the

Preprints (www.preprints.org) | NOT PEER-REVIEWED | Posted: 26 August 2020 doi:10.20944/preprints202008.0576.v1

first time. It allows one to describe the specific heat of solid phases from 0 K to melting points within experimental errors.

2. Relation of physicochemical constants of isostructural compounds using the Periodic Law.

The basis of this Law is the atomic number of the element (Z), which is equal to the number of protons in the atomic nucleus. This atomic number defines the chemical properties and most of the physical properties of the atom. This law can be extended and applied to different isostructural chemical compounds, both binary and multicomponent systems.

Let us consider, as an example, the heat capacity of diamond-like elements of the fourth group (C, Si, Ge, Sn) and their isostructural analogues of the $A^{III}B^{V}$ and $A^{II}B^{VI}$ phases ($Fd\bar{3}m$) in the solid state over a wide temperature range from 0 K to their melting points. It was found that the dependence of the heat capacities from 5 to 2000K follows certain regularity. Phases with the same sum of the atomic numbers of elements (Z), such as diamond and $B_{0.5}N_{0.5\ (cub)}$ (Z = 6); pure Si and $Al_{0.5}P_{0.5}$ (Z = 14); pure Ge and $Ga_{0.5}As_{0.5}$ (Z = 32)); pure grey α-Sn and $In_{0.5}Sb_{0.5}$, and $Cd_{0.5}Te_{0.5}$ (Z = 50) have the same heat capacity experimental values of the solid state within the experimental uncertainty.

3. The Hybrid Model of the Linear Combination of Debye's Functions and Mayer-Kelly Equation

The isochoric heat capacity C_v can be presented by the linear combinations of the Debye's functions [Debye, [3] and it is proposed to approximate the experimental data on the heat capacities of diamond-like phases in the form:

$$C_v(T, A_1, \Theta_1, A_2, \Theta_2, A_3, \Theta_3) = 3R \cdot (A_1 \cdot D(T/\Theta_1) + A_2 \cdot D(T/\Theta_2) + A_3 \cdot D(T/\Theta_3)) \quad (1)$$

Preprints (www.preprints.org) | NOT PEER-REVIEWED | Posted: 26 August 2020 doi:10.20944/preprints202008.0576.v1

$$D\left(\frac{T}{\Theta_j}\right) = 12\left(\frac{T}{\Theta_j}\right)^3 \int_0^{\Theta_j/T} \left(\frac{x^3}{(e^x-1)}\right) dx - 3\left(\Theta_j/T\right)\left(e^{\Theta_j/T} - 1\right), \quad (2)$$

D(T/Θj) – Debaye's function. With increasing temperature T, the specific heat C_v tends to 3R, and the Debye's functions tend to one.

R– gaz constant, *x* – dimensionless variable, j=1, 2, 3

$A_1 + A_2 + A_3 = 1$; A_1, Θ_1, A_2, Θ_2, A_3, Θ_3 – adjustable parameters.

To describe the solid state of the fourth group (C, Si, Ge, Sn) and some $A^{III}B^{V}$, $A^{II}B^{VI}$ compounds from 0 to 2000K the hybrid model of the linear combination of Debye's function and the Mayer-Kelly equation was proposed.

In this case, the function

$$C_p\,(T, T_o, a, b, A_1, \Theta_1, A_2, \Theta_2, A_3, \Theta_3) =$$

$$(a + bT/1000+(3R-a) / (1+T/T_o)^2)) \cdot C_v\,(T, A_1, \Theta_1, A_2, \Theta_2, A_3, \Theta_3) \quad (3)$$

T_o is an adjustable parameter that provides the smooth transition of heat capacity C_v to C_p in the equation (3) within a range from 1 to a coefficient b of the Mayer-Kelly equation.

The coefficients "a" and "b" were calculated with using the Mayer-Kelly equation:

$$C_p' = a + bT^{-3} + cT^{-2} \quad (4)$$

So C_p extends to C_v at low temperature, and it extends to the Mayer-Kelly equation at high temperatures. The least-squares m ethod is one of the common methods for the calculation of the minimum errors of deviation of approximate functions from experimental data.

$$\sigma^2\,(T_0, a, b, A_1, \Theta_1, A_2, \Theta_2, A_3, \Theta_3) = \sum_{i=1}^{n}(C_{p,calc} - C_{p,exp})^2/n \quad (5)$$

Here n is the number of experimental temperatures – heat capacity pairs of the selected phase (or phases).

Preprints (www.preprints.org) | NOT PEER-REVIEWED | Posted: 26 August 2020 doi:10.20944/preprints202008.0576.v1

The function σ (a, b, T_o, A_1, Θ_1, A_2, Θ_2, A_3, Θ_3) is a quadratic error between the experimental and the calculated values. The found parameters a, b, T_o, A_1, Θ_1, A_2, Θ_2, A_3, Θ_3, give the best approximation of the experimental data.

To describe the heat capacity, the in-house software on the base of commercial one DELPHI-7 was used with a 95% confidence level.

The selected values of heat capacities of the fourth group (C, Si, Ge, α-Sn and the analogue compounds AlP, GaAs, InSb, and CdTe, the range of temperatures and n number of the using points from the different references were collected in Tables 1-4.

Table 1. Selected values C_p for diamond and graphite

No	Phase	Reference	Number of points n	Temperature range
1	Diamond	[4]	107	$12.83 \leq T \leq 277.68$
2	Diamond	[5]	12	$298.15 \leq T \leq 500$
3	Diamond	[6]	16	$60 \leq T \leq 300$
4	Graphite	[7]	34	$1 \leq T \leq 1500$
5	Graphite	[8]	28	$200 \leq T \leq 2000$
6	Graphite	[9]	17	$200 \leq T \leq 1000$
7	Graphite	[10]	24	$100 \leq T \leq 2000$
8	Graphite	[11]	13	$300 \leq T \leq 2000$

Table 2. Selected values C_p for silicon and AlP

No	Phase	Reference	Number of points n	Temperature range
1	Si	[12]	16	$298.15 \leq T \leq 1000$
2	Si	[13]	101	$2.2 \leq T \leq 298.15$
3	Si	[14]	24	$5 \leq T \leq 300$
4	Si	[15]	12	$298,15 \leq T \leq 1400$
5	Si	[7]	30	$1 \leq T \leq 1400$
6	Si	[10]	17	$100 \leq T \leq 1600$
7	Si	[16]	15	$298.15 \leq T \leq 1673.150$
8	Si	[17]	12	$12 \leq T \leq 35$
9	Si	[18]	30	$14 \leq T \leq 270$
10	AlP	[19] exp	7	$800 \leq T \leq 1400$
11	AlP	[19] calc	8	$700 \leq T \leq 1400$
12	AlP	[20]	10	$500 \leq T \leq 1400$

Preprints (www.preprints.org) | NOT PEER-REVIEWED | Posted: 26 August 2020 doi:10.20944/preprints202008.0576.v1

Table 3. Selected values Cp for germanium and GaAs

No	Phase	Reference	Number of points n	Temperature range
1	Ge	21]	38	$20 \leq T \leq 200$
2	Ge	[14]	25	$2.5 \leq T \leq 300$
3	Ge	[22]	17	$5 \leq T \leq 160$
4	Ge	[23]	28	$310.8 \leq T \leq 762.9$
5	GaAs	[25]	19	$298.15 \leq T \leq 1400$
6	GaAs	[26]	35	$350 \leq T \leq 690$
7	GaAs	[27]	21	$12 \leq T \leq 273.2$

Table 4. Selected values Cp for α-Sn, InSb and CdTe

No	Phase	Reference	Number of points n	Temperature range
1	α-Sn	[29]	6	$1.5 \leq T \leq 4$
2	α-Sn	[22]	13	$7 \leq T \leq 100$
3	α-Sn	[30]	8	$12 \leq T \leq 273.2$
4	α-Sn	[7]	11	$3 \leq T \leq 100$
5	InSb	[31]	29	$6 \leq T \leq 100$
6	InSb	[27]	20	$12 \leq T \leq 273.2$
7	InSb	[28]	11	$350 \leq T \leq 800$
8	InSb	[32]	56	$2 \leq T \leq 750$
9	CdTe	[33]	10	$500 \leq T \leq 1400$

4. Results

The experimental data for the specific heat of C_p' compounds of diamond-like phases (at temperatures above 240 K) were processed by the least square method to obtain the coefficients a, b and c in the Mayer-Kelly formula. This formula is not applicable below 1200K for the diamond and cubic boron nitride. The calculated values of a, b and c are given in Table 5.

Table 5. Parameters of Mayer-Kelly equations $C'_p = a + b10^{-3}T - c10^5T^{-2}$ $(J/(mol\text{-}at)^{-1}\ K^{-1})$ at the high temperature region

No	Phase	a	b	c	T, K range	n	σ
1	Diamond [34]	22.43	0.0634	0.249	1200 - 2000	6	0.03
2	c-BN [34]	22.43	0.0634	0.249	1200 - 2000	6	0.03
3	Graphite	23.21	1.357	0,2993	1000 - 2000	35	0,07
4	Si	23,15	3,645	3,701	240 - 2000	86	0,12
5	Si, AlP	23,01	3,780	3,624	240 - 2000	111	0,16
6	Ge	23,51	3,667	1,205	240 - 2000	32	0,05
7	Ge, GaAs	23,37	3,853	1,115	240 - 2000	90	0,07
8	α-Sn, InSb, CdTe	24,33	4,768	0,737	240 - 2000	45	0.10

Preprints (www.preprints.org) | NOT PEER-REVIEWED | Posted: 26 August 2020 doi:10.20944/preprints202008.0576.v1

The calculated parameters a, b, T_o, A_1, Θ_1, A_2, Θ_2, A_3, Θ_3, the number of experimental pairs (TK- C_p) and standard errors are given in Table 6.

The coordinate of the minimum (σ) for the coefficients of the Debye's functions was taken from the regions of $0.01 < Aj < 1$, and $30\ K < \Theta j < 2000\ K$. The calculation was stopped when the heat capacity became equal to the mean-root-square error sigma (σ), with a value up to 0.05-0.15 J/(mole-at K) for a range of temperature from 0 to 2000K. The values of the heat capacities can be extended from 2000K to the melting point of every phase.

The main results were obtained by using the Hybrid Model of the Debye - Mayer-Kelly Equation. The remaining equations are auxiliary.

Table 6. Parameters of equation (3) in the range 0 K - T_m K

No	Phase	n	T_o	A_1	Θ_1	A_2	Θ_2	A_3	Θ_3	a	b	σ
1	Diamond	147	1202.4	0.393	1863.0	0.109	1849.2	0.499	1848.8	23.43	0.063	0.06
2	Graphite	116	606.1	0.769	2004.7	0.087	376.7	0.144	873.1	23,21	1.357	0,10
3	Si	282	489.5	0.352	340.0	0.371	825.1	0.278	858.6	23,15	3.645	0,08
4	Si+AlP	307	482.4	0.348	338,8	0.371	821.8	0.282	851.9	23,01	3.780	0.11
5	Ge	108	305.8	0.335	181.8	0.358	457.4	0.307	495.0	23,51	3.667	0.11
6	Ge, GaAs	183	292.8	0.335	181.0	0.358	454.0	0.308	490.3	23,37	3.853	0.16
7	α-Sn	38	243.6	0.341	96.4	0.398	299.8	0.261	308.5	24.33	4.768	0.12
8	α-Sn, InSb,CdTe	163	153.1	0.350	94.8	0.381	298.3	0.270	325.8	24.33	4.768	0.13
9	Ge, GaAs, AlSb,InP	297	325.7	0.356	165.4	0.333	486.1	0.311	524.3	23.15	3.716	0.35

Preprints (www.preprints.org) | NOT PEER-REVIEWED | Posted: 26 August 2020 doi:10.20944/preprints202008.0576.v1

Table 7. Parameters of polynomial equations $C_p = x_1T^3 + x_2 T^5 + x_3 T^6$ (J/(mol-at)$^{-1}$ K^{-1})

No	Phase	x_1	x_2	x_3	T_{min}, T_{max}	n	σ
1	Diamond	$2.317 \cdot 10^{-7}$	$5.765 \cdot 10^{-12}$	$-2.100 \cdot 10^{-14}$	0 - 250	111	0.02
2	c-BN [35]	$4.070 \cdot 10^{-7}$	$-1.752 \cdot 10^{-12}$	$6.839 \cdot 10^{-16}$	0 - 300	32	0.03
3	c-BN [34]	$4.758 \cdot 10^{-7}$	$-8.915 \cdot 10^{-13}$	$-3.756 \cdot 10^{-15}$	0 - 300	33	0.03
4	Graphite	$1.104 \cdot 10^{-5}$	$-7.128 \cdot 10^{-9}$	$8.664 \cdot 10^{-11}$	0 - 50	12	0.01
5	Si	$8.175 \cdot 10^{-6}$	$2.024 \cdot 10^{-8}$	$-3.301 \cdot 10^{-10}$	0 - 50	107	0.01
6	Ge	$1.456 \cdot 10^{-4}$	$-8.347 \cdot 10^{-8}$	$8.994 \cdot 10^{-10}$	0 - 50	26	0.07
7	Ge, GaAs	$1.478\ 10^{-4}$	$-8.557 \cdot 10^{-8}$	$9.293 \cdot 10^{-10}$	0 - 50	32	0.08
8	α-Sn	$8.405 \cdot 10^{-4}$	$-1.323 \cdot 10^{-6}$	$2.087 \cdot 10^{-8}$	0 - 20	20	0.06
9	α-Sn, InSb	$1.778 \cdot 10^{-4}$	$1.203 \cdot 10^{-5}$	$-6.573 \cdot 10^{-7}$	0 - 14	31	0.04

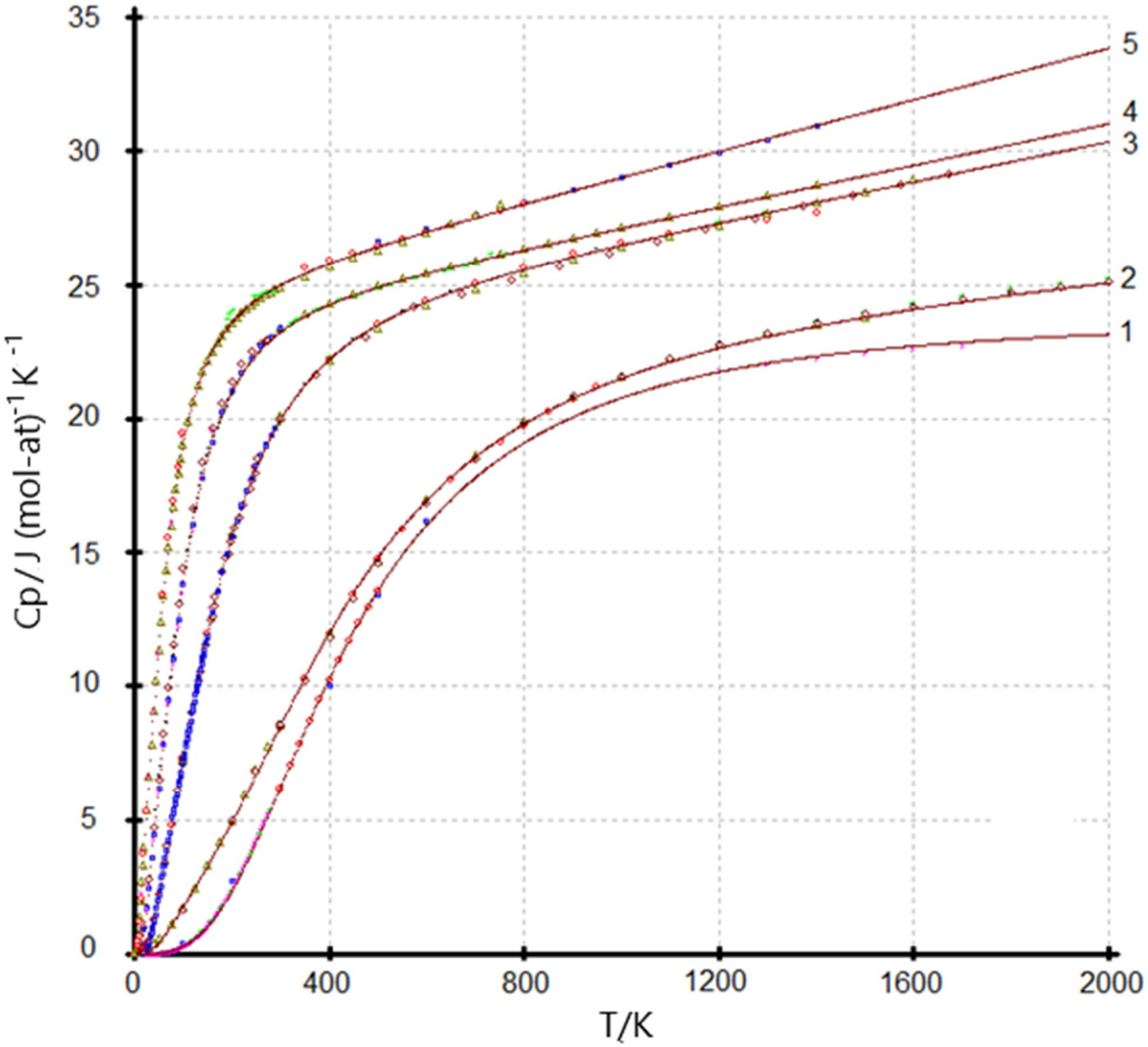

Fig. 1. A general trend of the heat capacities of fourth group elements and some $A^{II}B^{VI}$ and $A^{III}B^{V}$ phases. Selected values of the C_p (T) J/(mol-at)$^{-1}$ K^{-1}: 1-diamond and c-BN (compilation data); 2-graphite and h-BN; 3-Si and AlP; 4-Ge and GaAs; 5- α-Sn and InSb, and CdTe (See Table 1-6); 790 points

Preprints (www.preprints.org) | NOT PEER-REVIEWED | Posted: 26 August 2020 doi:10.20944/preprints202008.0576.v1

The heat capacities of the fourth group phases (in J/mole-at K) obtained by using the Debye-Mayer-Kelly equation (3) are presented in Table 8 within the range of temperature 5 – 300 K. (See the columns II, III-VI, and equations 1, 2, 4, 6, 8 from Table 6.)

Table 8. The calculated heat capacities (J/(mol-at)$^{-1}$ K^{-1}) of the fourth group phases See Fig. 1, Table 6 (eq. 1, 2, 4, 6, 8) and Table 7 (eq. 1)

T, K	Diamond & c-BN Curve 1, Fig.1	Diamond & c-BN See eq.1 Table 7	Grapite & h-BN Curve 2, Fig.1	Si Curve 3. Fig.1	Ge & Z=32 Curve 4, Fig.1	α-Sn & Z=50 Curve 5, Fig.1
I	II	III	IV	V	VI	VII
5	0.00004	0.00003	0.0005	0.0024	0.0153	0.098
10	0.0003	0.00023	0.0038	0.0195	0.1222	0.762
15	0.0010	0.0008	0.0127	0.0660	0.4102	2.122
20	0.0024	0.0018	0.0302	0.1564	0.9352	3.702
25	0.0047	0.0037	0.0589	0.3051	1.6712	5.201
30	0.0082	0.0064	0.1015	0.5233	2.5364	6.580
35	0.013	0.010	0.1597	0.8154	3.4561	7.880
40	0.019	0.015	0.2337	1.1777	4.3868	9.129
45	0.028	0.022	0.323	1.599	5.309	10.332
50	0.038	0.030	0.425	2.065	6.215	11.482
60	0.07	0.054	0.66	3.08	7.98	13.59
70	0.10	0.087	0.92	4.14	9.65	15.40
80	0.16	0.13	1.19	5.21	11.22	16.92
90	0.22	0.19	1.47	6.26	12.66	18.18
100	0.30	0.27	1.76	7.29	13.97	19.22
110	0.41	0.36	2.05	8.29	15.13	20.08
120	0.53	0.48	2.34	9.27	16.16	20.79
130	0.67	0.62	2.65	10.2	17.07	21.39
140	0.83	0.79	2.95	11.11	17.87	21.89
150	1.02	0.98	3.26	11.96	18.57	22.32
160	1.24	1.20	3.58	12.78	19.19	22.69
170	1.48	1.45	3.91	13.54	19.73	23.01
180	1.74	1.73	4.24	14.27	20.21	23.29
190	2.02	2.03	4.57	14.94	20.63	23.54
200	2.33	2.35	4.91	15.58	21.01	23.75
210	2.66	2.70	5.26	16.17	21.35	23.95
220	3.01	3.06	5.61	16.72	21.65	24.13
230	3.38	3.42	5.97	17.23	21.92	24.29
240	3.76	3.78	6.33	17.71	22.16	24.43
250	4.15	4.12	6.69	18.15	22.38	24.57
260	4.55	No	7.06	18.57	22.58	24.69
280	5.38	valuable	7.79	19.32	22.94	24.91
300	6.23		8.53	19.96	23.24	25.11

Preprints (www.preprints.org) | NOT PEER-REVIEWED | Posted: 26 August 2020 doi:10.20944/preprints202008.0576.v1

We also calculated the heat capacities of diamond and cubic boron nitride using the polynomial equation 1 (Table 7), which are presented in column III (Table 8).

The values of columns II and III are consistent with each other within the range of experimental error. The heat capacities above 300 K can be determined with equation (3) or Mayer-Kelly equations (4) (Table 5).

5. Discussion. The heat capacity measurements and sources of errors.

5.1. Diamond and c-BN; graphite and h-BN

The investigation of the heat capacities of systems based on light elements such as lithium, beryllium, boron, and carbon is an extremely complex experimental task. The presence of impurities or variations in the isotopic composition has a stronger effect on the physicochemical properties than on the heavy elements.

Diamond and cubic boron nitride have the same crystal structure of the type ($Fd\bar{3}m$). Both substances are in a metastable state under normal conditions. In accordance with the concept of similarity put forward by us, isostructural substances with the same sum of atomic numbers have the same heat capacities within the experimental errors per J (mol-at)$^{-1}$ K^{-1}. The purity of the substance is the most important characteristic in the study of heat capacity. Synthetic diamond and various modifications of boron nitrides (cubic, wurtzite, hexagonal, rhombohedral, turbostratic) [34] contain various impurities due to the specifics of their synthesis [36].

So, it was found in [21], when studying the influence of the alloying additives on the heat capacity of germanium at temperatures of 20 –200 K, that the heat capacity of

Preprints (www.preprints.org) | NOT PEER-REVIEWED | Posted: 26 August 2020 doi:10.20944/preprints202008.0576.v1

germanium with an aluminum content of up to 0.006 at.% gives an increase of 0.17 J/(mol-at)$^{-1}$ K^{-1} at temperature of 100 K compared to pure germanium (See Fig.3).

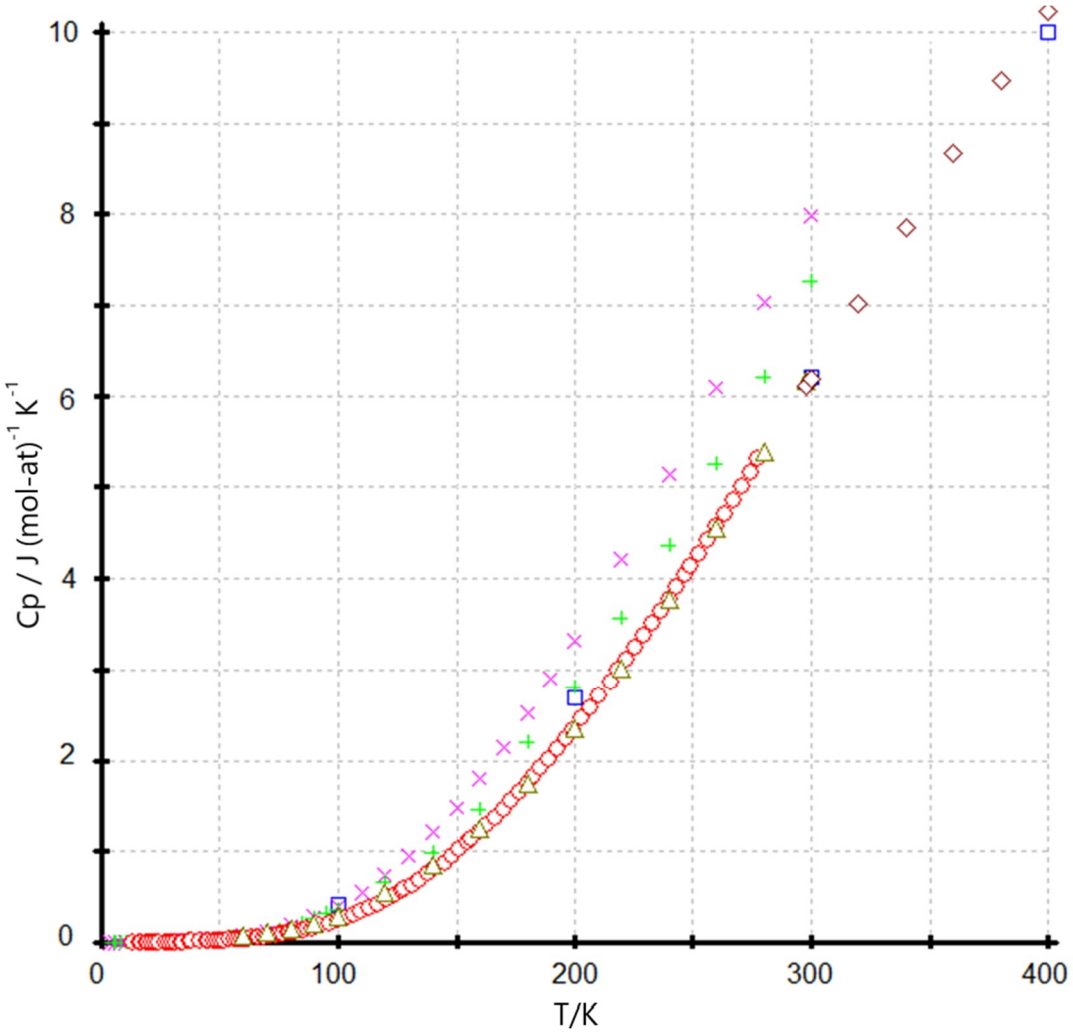

. **Fig. 2.** Comparison of the heat capacities of cubic boron nitride c-BN (□ [37], × [34], + [35]; and diamond (○ [4], △ [6], ◇ [5]

The heat capacity of diamond was studied on industrial samples with a content of 0.2 wt. % in [4, 5] and up to 1 wt. % of impurities in [6].

It was noted in [35] that cubic boron nitride used in the measurements contained up to 4 wt. % hexagonal boron nitride and up to 1% metallic impurities. According to [34], cubic BN included up to 0.15 wt. % impurities. Nevertheless, the low-temperature heat capacities of cubic BN [35] are closer to the heat curve of diamond than the data of [34].

Preprints (www.preprints.org) | NOT PEER-REVIEWED | Posted: 26 August 2020 doi:10.20944/preprints202008.0576.v1

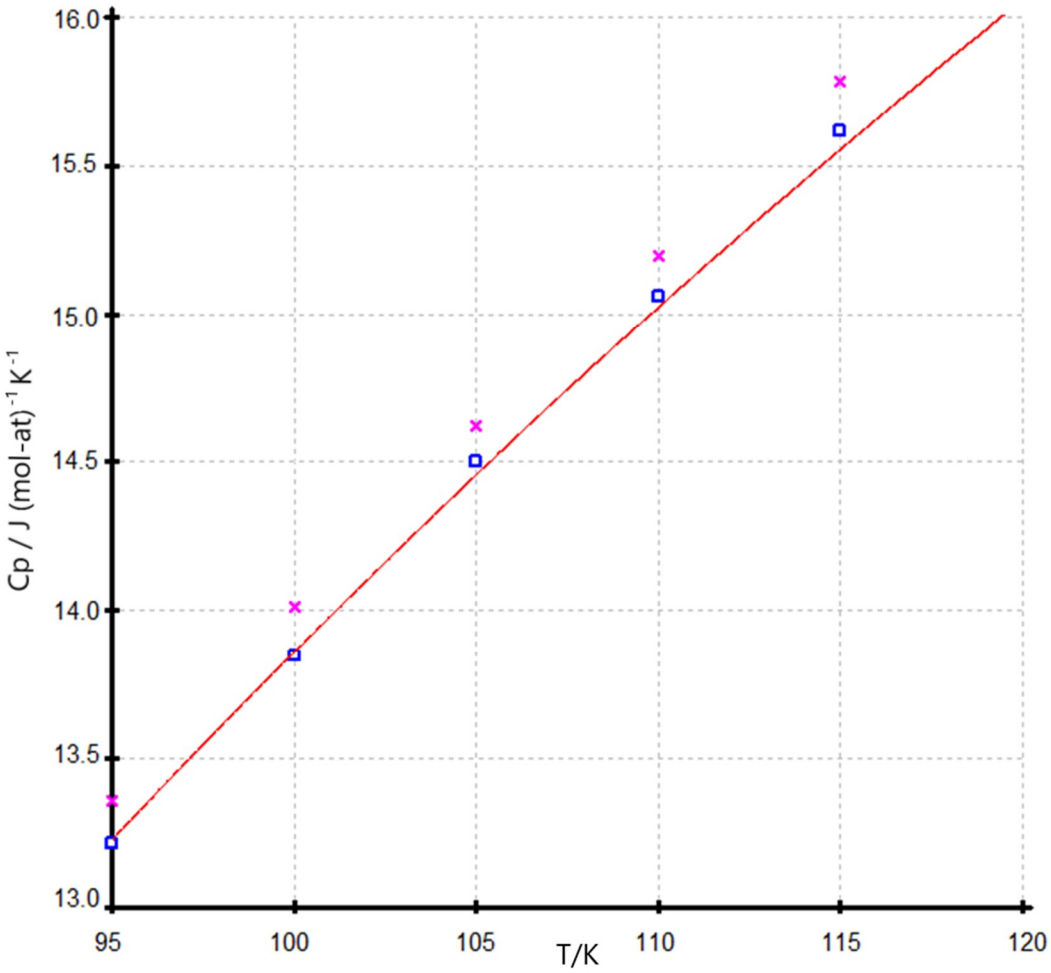

Fig. 3. Comparison of the heat capacity: □ - pure Ge [21], × - Ge with 0.006 at %Al [21], line is a fitted Ge (Table 6).

Today the company Intelligent Material Pvt. Ltd fabricates the cubic boron nitride of the purity up to 99% with APS: 80-120 nm. The C_p of this product is variated in the range 10.4 – 19.9 J/(mol-at)$^{-1}$ K^{-1} and the value of the C_p is higher than C_p (c-BN) = 8 J/(mol-at)$^{-1}$ K^{-1} and C_p (h-BN) = 10.0 J/(mol-at)$^{-1}$ K^{-1} [34]. It is clear that such heat capacity values are associated with finely dispersed c-BN particles.

The recent calculated results of the specific heat of cubic BN by the Monte Carlo method [37] showed good agreement with the specific heat of diamond [4, 5, 6, 10] in the range of 100-600K (see Fig.2).

The issue of low-temperature graphitization remains open. In the absence of oxygen, the diamond can be heated to about 2000 K. However, the surface of the diamond is covered

Preprints (www.preprints.org) | NOT PEER-REVIEWED | Posted: 26 August 2020 doi:10.20944/preprints202008.0576.v1

with a layer of graphite [38]. The presence of impurities can contribute to the catalytic graphitization of diamond. In [39] the kinetics of graphitization of thin diamond-like carbon (DLC) films was studied at 773K coated with Ni metallic nanoparticles [39]. Among the three low index planes, the {111} plane can be graphitized easily [39].

In [5] while measuring the heat capacity of diamond a silver container was used. Silver, its vapors and impurities up to 0.2% can contribute to the graphitization of diamond above 800 K.

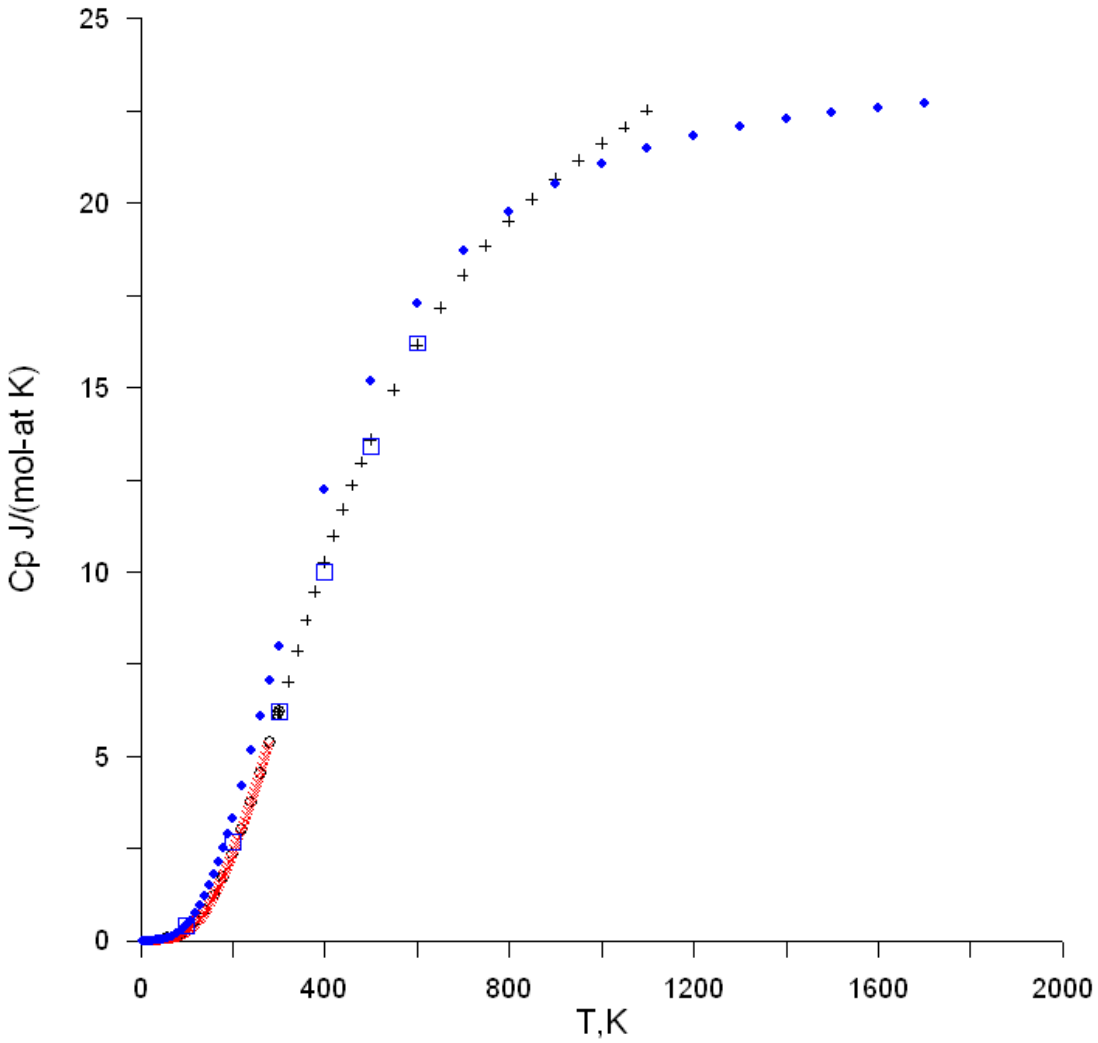

Fig. 4. Comparison of the heat capacities C_p (T) of diamond 1 (+ [5], ○ [6], × [4]) and cubic boron nitride 2 (• [34], □ [37]).

In Fig. 4, the heat capacity of diamond (1) with points + [5] intersects the heat capacity c-BN (2) [34] and goes into the heat capacity region of graphite above 800 K (compare with

Preprints (www.preprints.org) | NOT PEER-REVIEWED | Posted: 26 August 2020 doi:10.20944/preprints202008.0576.v1

Fig. 1), which contradicts commonly accepted beliefs. The compiled heat capacity curve of the diamond was shown in Fig. 5. This curve of the diamond was described by equation (3), the parameters of which are presented in Table 6.

According to our concept, there should be no overlap of the heat capacity curves, since all isostructural phases form independent groups in accordance with the sum of the atomic numbers of the elements or the structure of the phases. Let us compare the heat capacities of graphite and hexagonal boron nitride [34], although the data [34] are unreliable due to the presence of impurities. According to our concept, hexagonal boron nitride should have a specific heat capacity similar to graphite.

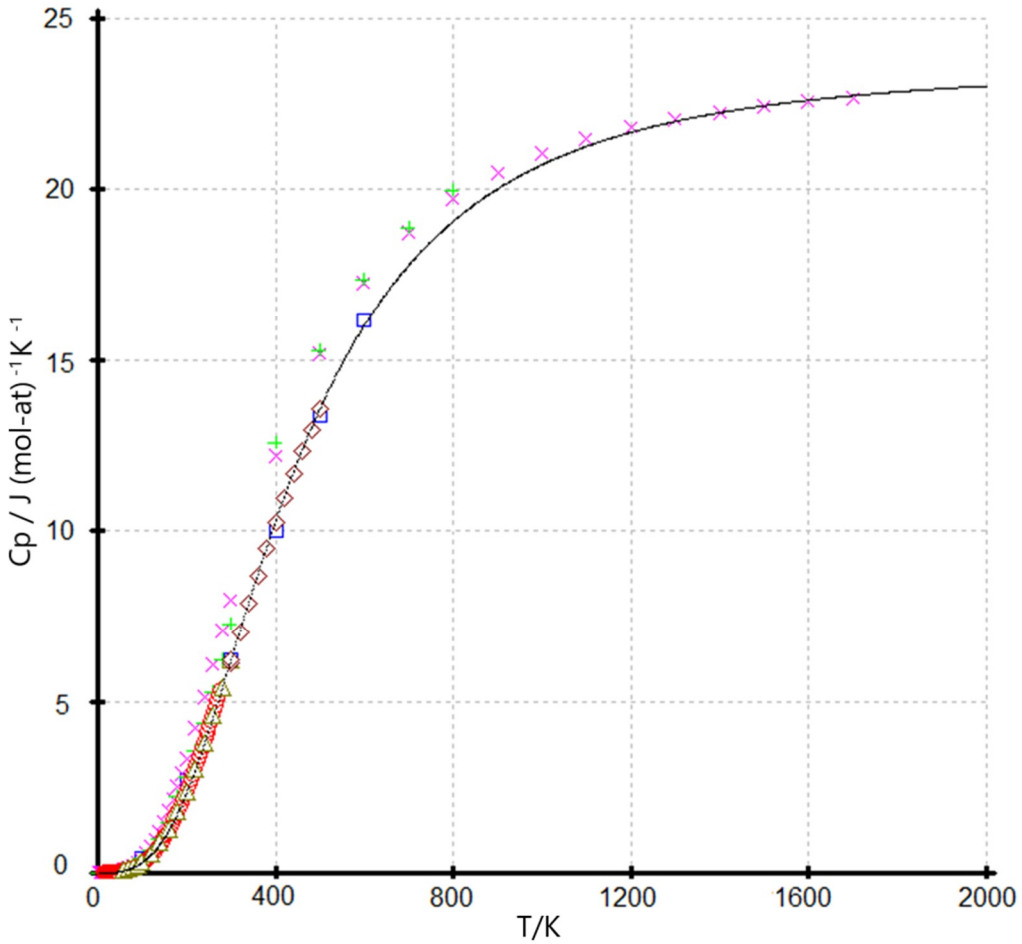

Fig. 5. Comparison of the heat capacities (points) of cubic boron nitride c-BN (□ [37], × [34], + [35]; and diamond (○ [4], △ [6], ◇ [5]; solid line is a compiled curve C_p (T) of diamond.

Preprints (www.preprints.org) | NOT PEER-REVIEWED | Posted: 26 August 2020 doi:10.20944/preprints202008.0576.v1

It is necessary to note that the data [34] of the heat capacities of cubic boron nitride begin to correspond to diamond and that of hexagonal boron nitride to graphite at temperatures above 1000K. In our opinion, the impurity of the samples ceases to affect the measured heat capacity due to their removal from the container at high temperatures and the transformation of a substance in a normal state.

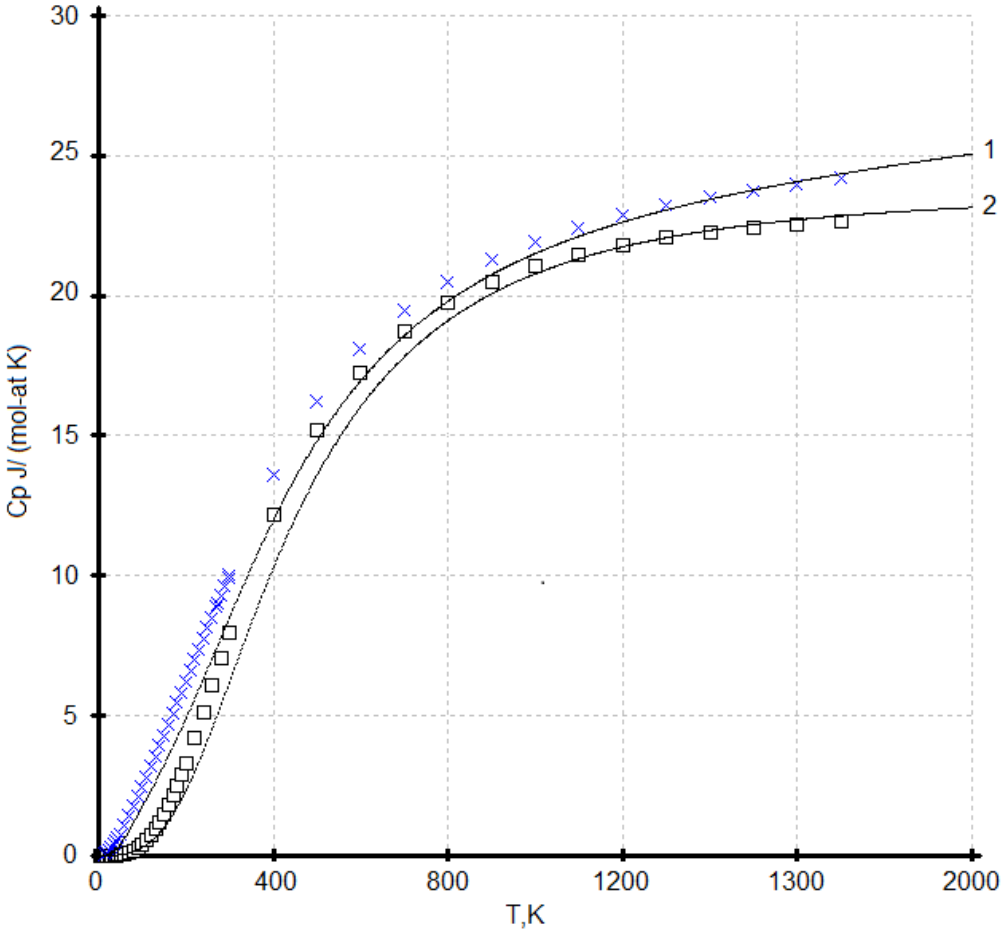

Fig. 6. Comparison C_p data of diamond, cubic boron nitride, graphite and hexagonal boron nitride. Points □ c-BN [34], × h-BN [34]; Calculated values C_p (T): 1 –graphite, 2- diamond (see Table 1 and 6)

5.2. Silicon and AlP

When analyzing the capacity of silicon, the following sources were used [7, 10, 12, 13, 14, 15, 16, 17, 18) (see Tables 2, 5, 6 and Fig.1). All cited results of the heat capacity of silicon in solid state was described by equation (4) with precision σ=0.08 J/(mol-at)$^{-1}$ K^{-1}

Preprints (www.preprints.org) | NOT PEER-REVIEWED | Posted: 26 August 2020 doi:10.20944/preprints202008.0576.v1

in the range of temperature 5 – 2000 K. Below 50 K the heat capacity of silicon is described well by polynomial equation $C_p = x_1T^3 + x_2T^5 + x_3T^6$ with error $\sigma = 0.01$ J/(mol-at)$^{-1}$ K^{-1} (See Table 7).

Aluminum phosphide is a highly toxic substance; contact with water or moist air releases toxic phosphine [40]. That is why the study of its physicochemical properties is limited. The heat capacity of aluminum phosphide was studded in [19], [20] at high temperature (See Table 2, 5, 6). We did not use the heat capacity data of the $A^{III}B^{V}$ compounds [20] due to their high error. Nevertheless, in some cases, in the absence of other data, they can be used. So, the heat capacity data [20] showed satisfactory agreement when optimizing the Al-P system in [41].

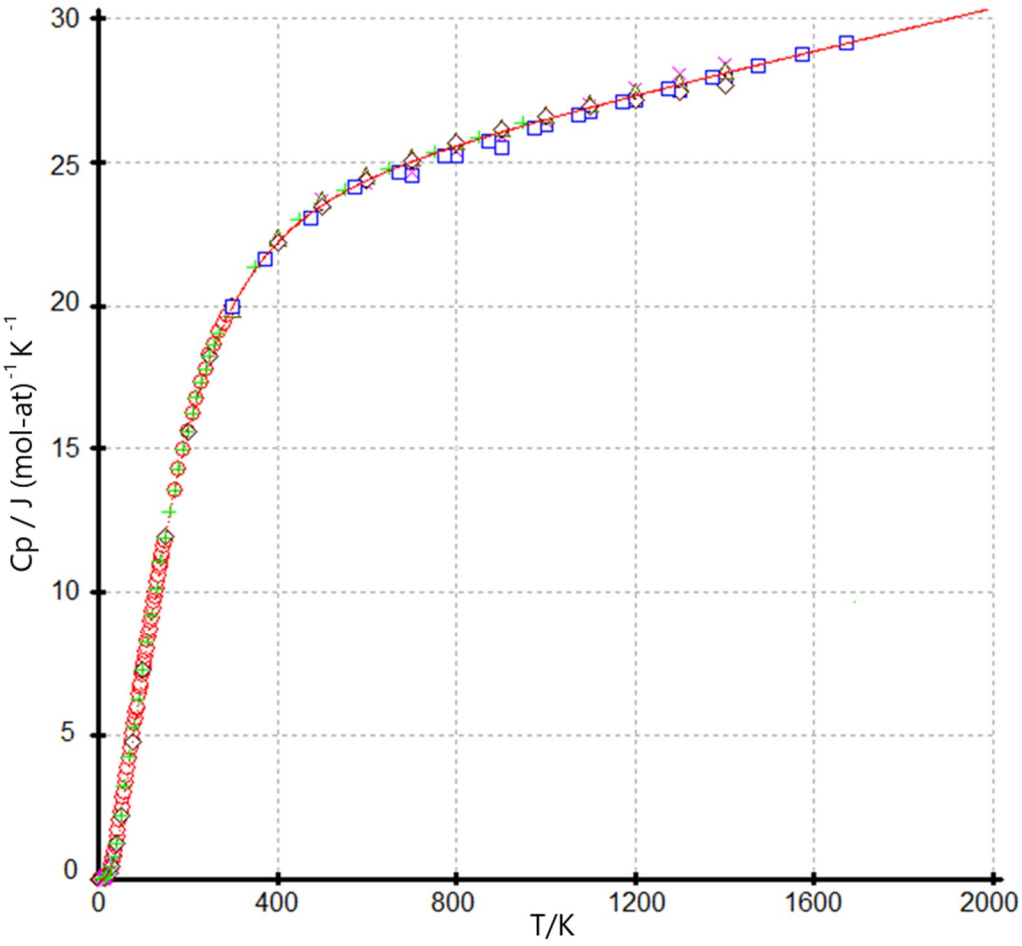

Fig. 7. Heat capacity Cp (T) of the silicon and AlP. Experimental points of Si: + [12], ○ [13], △ [15], ◇ [7], •[10], □ [16], × [17], + [18]; AlP: □ [19], × [20]

Preprints (www.preprints.org) | NOT PEER-REVIEWED | Posted: 26 August 2020 doi:10.20944/preprints202008.0576.v1

According to our concept of equal heat capacities of isostructural phases with the same sum of atomic numbers of elements per one mole-atom of a substance, it follows that the heat capacities of silicon and aluminum phosphide should not differ within experimental errors. So, the heat capacity data of aluminum phosphide should be the same as for silicon for the range of temperature from 0 to 2000 K.

Earlier, we evaluated the heat capacity of AlP using the linear correlation of C_P (T) vs. logarithm of the sum of atomic numbers of elements for the $A^{III}B^{V}$ phases of the sphalerite type at 298–1000 K [Vas13]. Unfortunately, the proposed linear correlation is not applicable to compounds with a small sum of atomic numbers Z = 14 (as AlP), but is valuable for compounds starting from the sum of atomic numbers Z = 23 as AlAs and GaP) per mole-atom.

5.3. Germanium and GaAs

The selected values of the heat capacity of germanium and GaAs were taken from the following references: [14, 21, 22, 23, 24] and [25, 26, 27], respectively.

The experimental points of the heat capacity of silicon C_p (T) in the solid state was described by equation (4) with precision σ= 0.11 J/(mol-at)$^{-1}$ K^{-1} in the range of temperature 5 – 2000 K. Parameters of this equation were presented in Table 6. Below 50 K the heat capacity of germanium were described by the polynomial equation $C_p = x_1T^3 + x_2T^5 + x_3T^6$ with error σ= 0.07 J/(mol-at)$^{-1}$ K^{-1} (See the Table 7).

The set of experimental points of the heat capacity of Ge and GaAs C_p (T) was described by equation (4) with precision σ= 0.16 J/(mol-at)$^{-1}$ K^{-1} and by polynomial equation with precision σ= 0.08 J/(mol-at)$^{-1}$ K^{-1} in the same range of temperature.

Preprints (www.preprints.org) | NOT PEER-REVIEWED | Posted: 26 August 2020 doi:10.20944/preprints202008.0576.v1

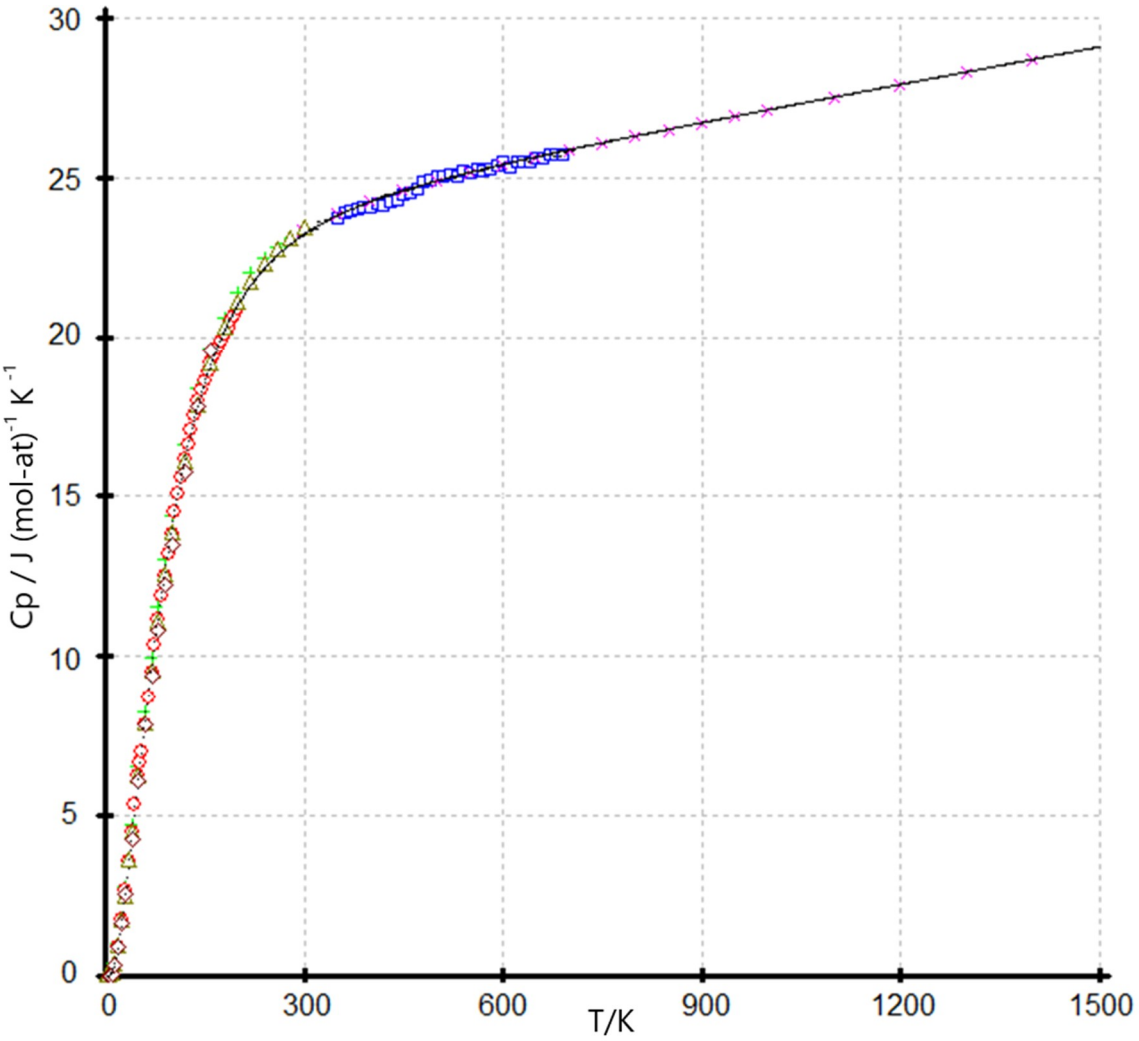

Fig. 8. Heat capacity C_p (T) of the germanium and GaAs. Experimental points of Ge: ○ [21], △ [14], ◇ [22], • [24]; + [12]; AlP: □ [25], × [25], + [27]. Calculated C_p (T) – solid line.

The AlSb, InP, CdS, and ZnSe compounds with a sum of atomic numbers 32 per mole-atom have a C_p (T) dependence close to that of germanium. The discrepancy error of heat capacity may be associated with a deviation from the stoichiometry of the forming phases [43, 44] and the influence of impurities [21] (see Fig.3) as well as the difference in the isotopic composition of elements [45, 46, 47]. There is also a great influence of the high partial pressure of the vapor components of the substance on the heat capacity at high temperature.

Preprints (www.preprints.org) | NOT PEER-REVIEWED | Posted: 26 August 2020 doi:10.20944/preprints202008.0576.v1

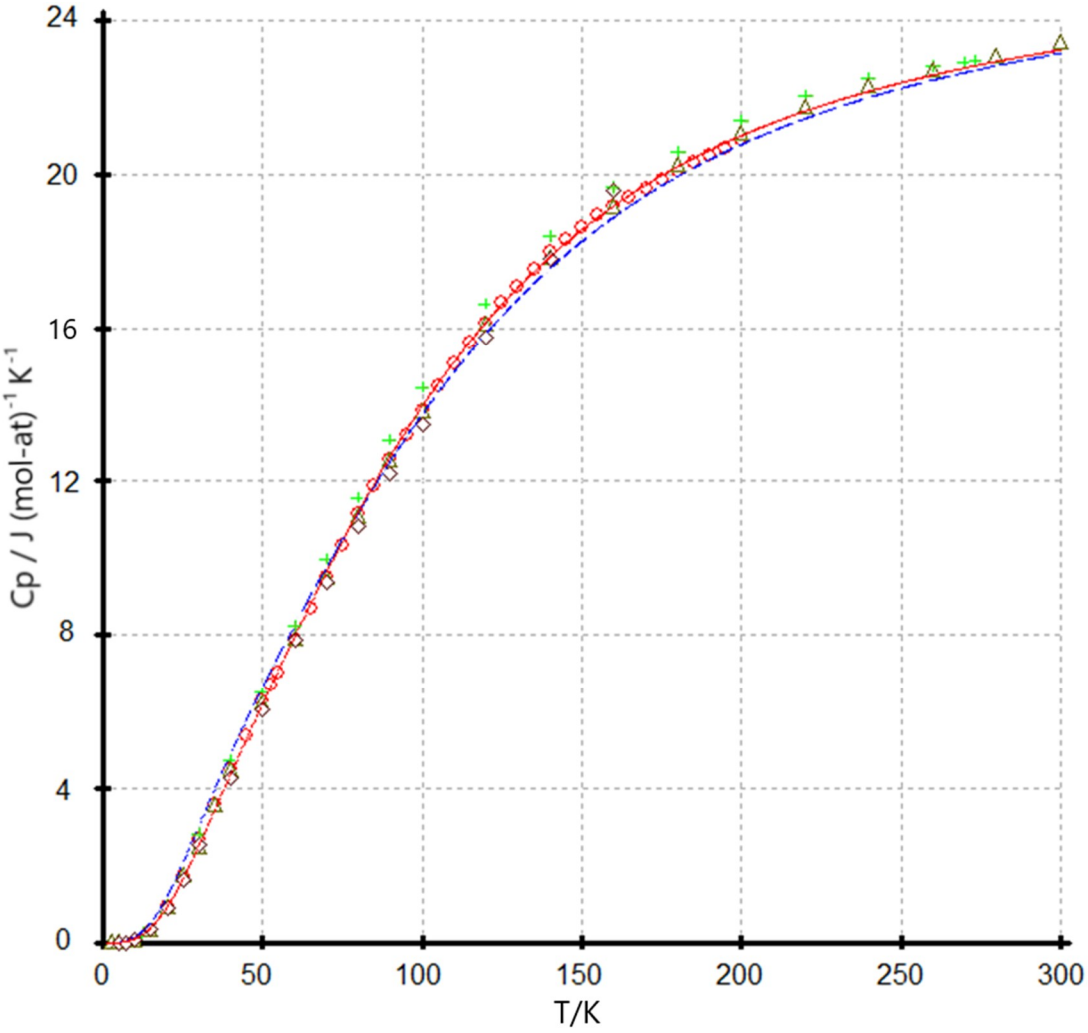

Fig. 9. Comparison of the heat capacities Cp (T) curves germanium (with experimental points of germanium: ○ [21], △ [14], ◇ [22]) – solid red line, and dash blue line with the virtual points Ge, GaAs, AlSb, InP.

The heat capacity of indium phosphide at high temperatures was studied in three papers (See Table 9 and Fig.10)

Table 9. Parameters $C_p = a+b10^{-3}T-c10^5T^{-2}$ (J/(mol-at)$^{-1}$ K^{-1}) of the InP phase

a	b	c	T, K range	Method	Reference
50.10	5.07	5.01	700 - 1000	Drop-calorimetry	[20]
53.69	-1.57	7.3	350 - 750	DSC	[48]
51.34	-	4.77	350 - 750	DSC	[49]

Preprints (www.preprints.org) | NOT PEER-REVIEWED | Posted: 26 August 2020 doi:10.20944/preprints202008.0576.v1

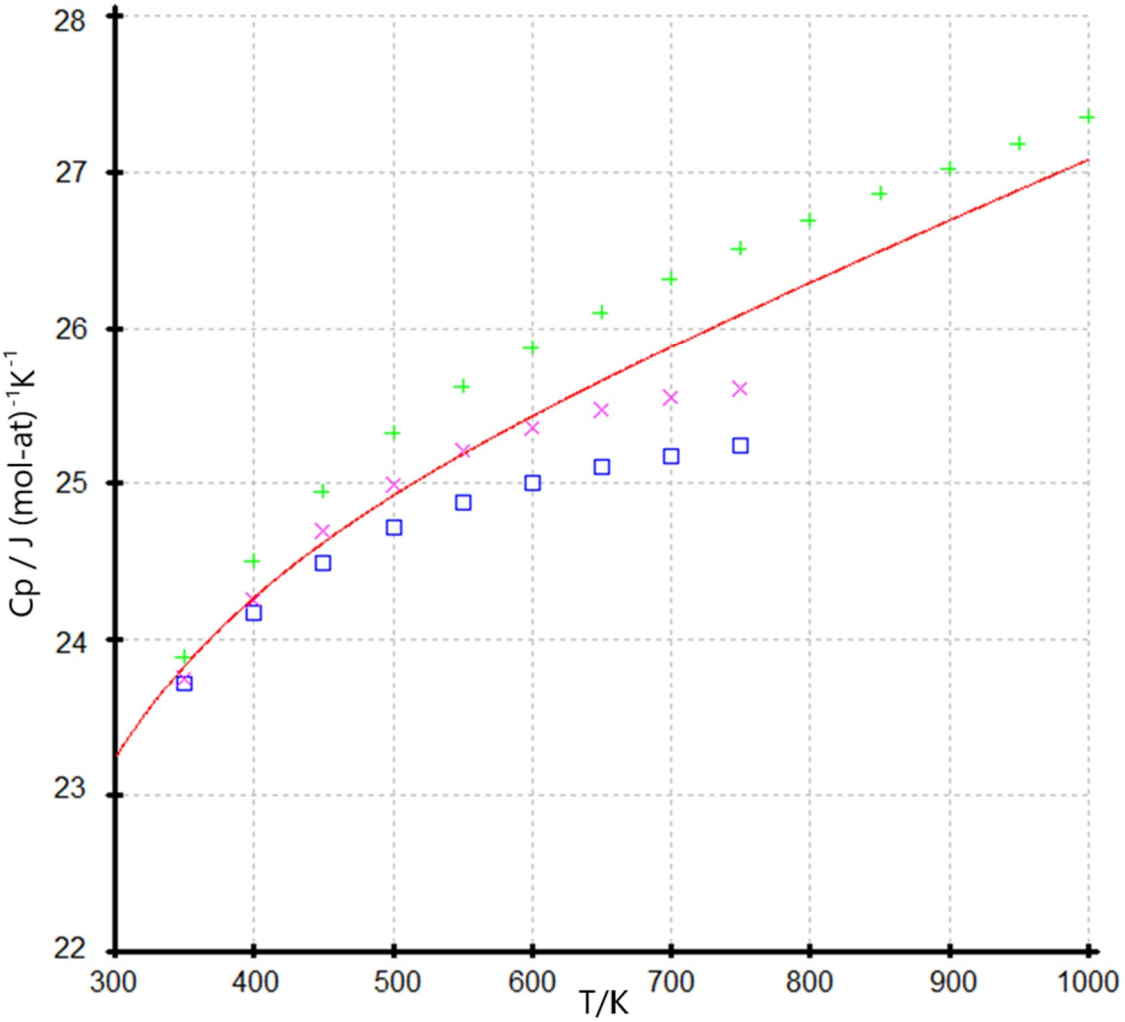

Fig. 10. Comparison of the heat capacities Cp (T) of the InP phase (points: + [20], × [48], □ [49], and germanium (solid red line) (see Table 6).

If the low-temperature heat capacities of germanium and indium phosphide are in good agreement with each other, their high-temperature values are contradictory. Variants of the DSC method [48, 49] are not suitable for studying the heat capacity of indium phosphide due to the high partial pressure of phosphorus at high temperatures (see Fig. 11). Drop calorimetry data of the AIIIBV compounds in [20] are usually overestimated. Therefore, the high-temperature heat capacities of indium phosphide were not used in our calculations.

Preprints (www.preprints.org) | NOT PEER-REVIEWED | Posted: 26 August 2020 doi:10.20944/preprints202008.0576.v1

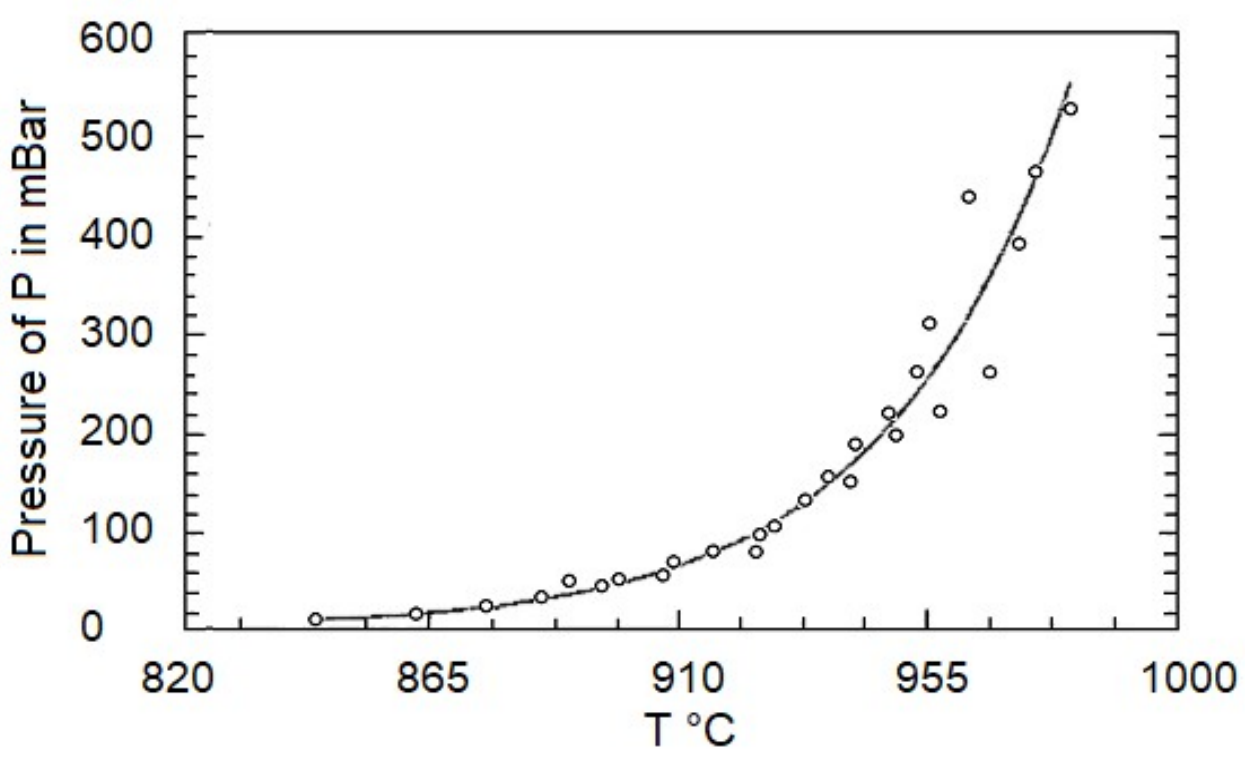

Fig. 11. Pressure of phosphorus in equilibrium with solid InP [50]

5.4. Grey tin (α-Sn), InSb and CdTe

We analyzed the following references of heat capacities of gray tin (α-Sn) [7, 22, 29, 30]; InSb [27, 28, 31, 32] and CdTe [33] (see Tables 2, 5-7, and Fig.1).

The experimental points of the heat capacity C_p (T) of α-Sn in solid state was described by equation (3) with precision σ= 0.12 J/(mol-at)$^{-1}$ K^{-1} in the range of temperature 5 – 2000 K. Parameters of this equation are presented in Table 6. Below 14 K the heat capacity of gray tin were described by the polynomial equation $C_p = x_1T^3 + x_2T^5 + x_3T^6$ with error σ= 0.03 J/(mol-at)$^{-1}$ K^{-1} (See the Table 7). The calculated values of gray tin above 287.15 K correspond to its metastable state.

The heat capacities of InSb and CdTe are the same as the gray tin below 287.15 K within the limitation of the experimental data.

Preprints (www.preprints.org) | NOT PEER-REVIEWED | Posted: 26 August 2020 doi:10.20944/preprints202008.0576.v1

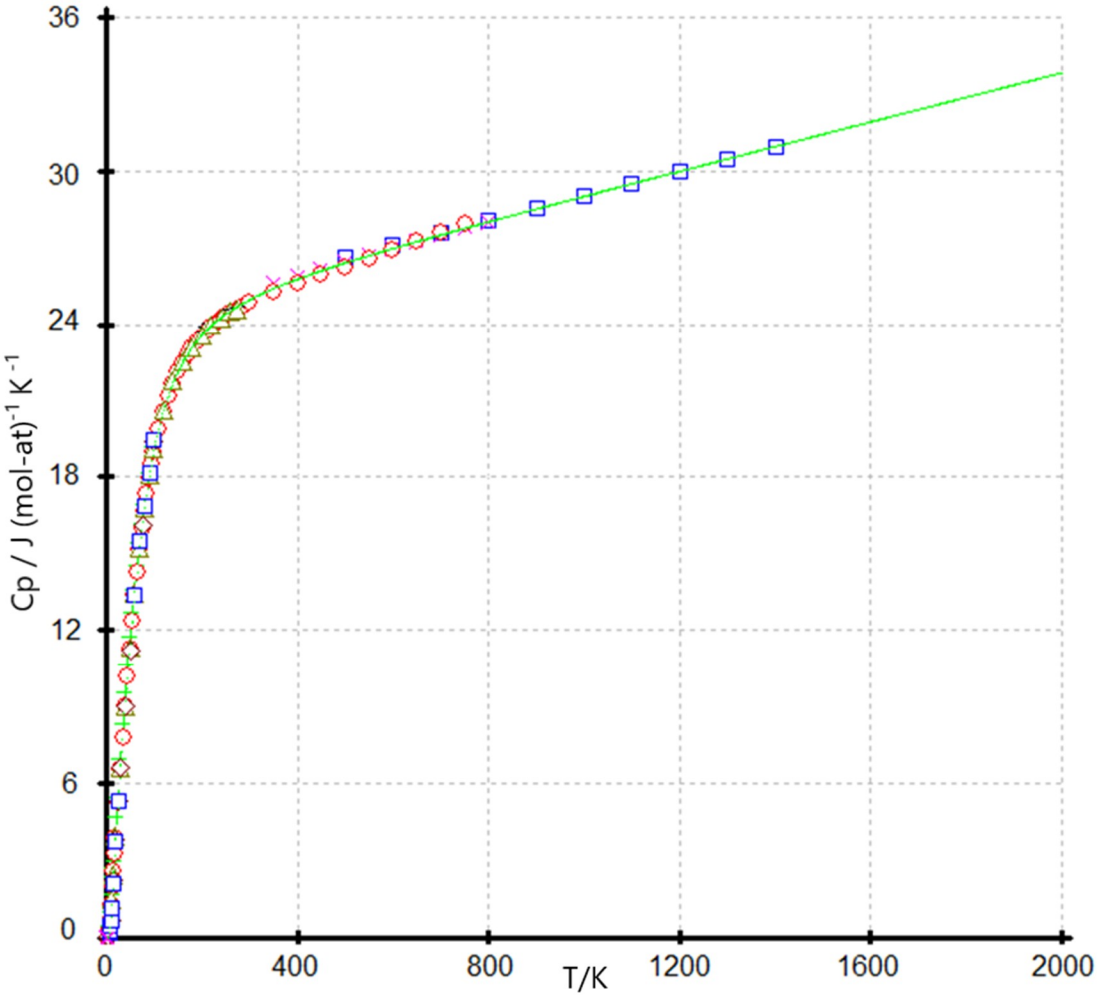

Fig. 12. Heat capacity C_p (T) of the (α-Sn): × [29], □ [22], • [30], ◇ [7]; + InSb [31], △ [27], × [28], ○ [32] and □ CdTe [33]

The Table 10 contains the standard thermodynamic values of the fourth group elements of Periodic table and diamond-like $A^{III}B^{V}$ and $A^{II}B^{VI}$ compounds: cubic BN, AlP, GaAs, AlSb, InP, InSb, CdTe in comparison with the electronic handbook [51].

At present, low-temperature calorimetry allows one to obtain heat capacity with high accuracy. The occurrence of the discrepancy among the results is primarily associated with the purity of the sample, by the sorption of atmospheric gases and moisture, or the presence in the studied sample of concomitant impurities of other allotropic modifications and isotopic difference of the specimens.

Preprints (www.preprints.org) | NOT PEER-REVIEWED | Posted: 26 August 2020 doi:10.20944/preprints202008.0576.v1

The compounds with the sum of atomic numbers Z = 19 $Ga_{0.5}N_{0.5}$ and $B_{0.5}As_{0.5}$ are not considered in this paper. In addition, they have other spatial groups: $A^{III}N$ ($P6_3mc$) and $B_{0.5}P_{0.5}$, and $B_{0.5}As_{0.5}$ ($F\bar{4}3m$).

Table 10. Standards thermodynamic values of the fourth group elements of Periodic Law and certain diamond-like $A^{III}B^{V}$ and $A^{II}B^{VI}$ compounds

Phase	Tm, K	Cp_{298} J/(mol-at)$^{-1}$K^{-1}	S_{298} J/(mol-at)$^{-1}$ K^{-1}	H_{298}-H_o J/(mol-at)$^{-1}$K^{-1}	G_{298} J/(mol-at)$^{-1}$K^{-1}	Reference
Diamond	*	6.12±0.04	2.37±0.02	519 ±4		[51]
Diam., BN-c	**	6.15±0.04	2.40±0.02	528 ±4	191±3	This work
Graphite,	4800±200	8.53±0.2	5.74±0.13	1050±21		[51]
BN-h	**	8.46±0.2	5.60±0.15	1042±15	-629±1	This work
Si	1688±3 [51]	20.04±0.04	18.83±0.1	3213.3±4		[51]
Si & AlP	AlP: 2823 [41]	19.91±0.15	18.80±0.15	3206.2±4	-2385±4	This work
Ge	1210.4±0.5	23.39±0.1	31.13±0.15	4640±20		[51]
	[51]	23.21±0.1	31.0±0.13	4618.9±5	-4638±5	This work
GaAs	1511±2 [51]	23.43±0.8	32.09±0.2	4727.9±20		TKB
Ge & GaAs		23.2±0.14	31.2±0.17	4633.8±5	-4669±5	This work
AlSb	1333±3 [51]	23.16±0.6	32.13±0.3	4617±20		[51]
InP	1328±5 [51]	22.76±0.1	31.38±0.4	4497.8±42		[51]
Z= 32		23.12±0.7	31.6±0.8	4611.1±15	-4799 ±15	This work
α-Sn	T_{tr} α-, β-Sn	25.77±0.15	44.14±0.2	5757±40		[51]
	287.15	25.1±0.24	43.8 ±0.4	5664.3±40	-7405±40	This work
InSb	798.4±0.3 [51]	24.7±0.11	43.55±0.42	5652±50		[51]
CdTe	1365±5 [51]	25.08±0.15	47.49±0.40	5209±50		[51]
Z =50		24.96±0.13	43.70±0.2	5628.4±40	7414±40	This work

Conclusion

The carried out thermodynamic analysis showed that the series of considered isostructural substances consist of five groups:

1) diamond and cubic boron nitride c-$B_{0.5}N_{0.5\,(cub)}$ (Z = 6);
2) graphite and hexagonal boron nitride h-$B_{0.5}N_{0.5}$ (Z = 6);
3) pure Si and $Al_{0.5}P_{0.5}$ (Z = 14);
4) pure Ge and $Ga_{0.5}As_{0.5}$, $Al_{0.5}Sb_{0.5}$, $In_{0.5}P_{0.5}$ (Z = 32));

Preprints (www.preprints.org) | NOT PEER-REVIEWED | Posted: 26 August 2020 doi:10.20944/preprints202008.0576.v1

5) pure gray α-Sn and $In_{0.5}Sb_{0.5}$, and $Cd_{0.5}Te_{0.5}$ (Z = 50)

Z – atomic number of one mole-atom substance

The heat capacity of every group of substances in solid state with the same atomic number has the same values $C_p(T)$ in the range of temperature from 0 to melting point (T_m). Heat capacities were calculated using the hybrid model of a linear combination of the Debye functions and Mayer-Kelly equation. There is no a similar model description in literature. The researchers still have not found a suitable model for describing the heat capacity from 0 K to the melting point [54].

The error of the calculated heat capacities does not exceed the error in measurements of an experimental one. For each group of the analyzed phases with the same atomic number (Z), it is preferable to use the heat capacity of pure elements, which should be considered as standard substances.

Our proposed model eliminates all the shortcomings of the description when extrapolating data. The reliable heat capacity data are required in industry for growing single crystals and films.

The model can be used in both binary and multicomponent systems of different substances. This model also helps the standardization of physicochemical constants.

This work is indispensable for both the prognostic calculations in the chemical thermodynamics and applied research projects.

Acknowledgements:

We would like to thank Prof. Lorie Wood from the University of Colorado (USA) for the language help.

References:

[1] Vassiliev, V.P.; Legendre, B.; Zlomanov, V.P. The critical analysis and mutual coherence of thermodynamic data of the AIIIBV phases. *Intermetallics* **2011**, *19*, 1891-1901. https://doi.org/10.1016/j.intermet.2011.07.023

[2] Vassiliev, V.P.; Taldrik, A.F.; Ilinykh, N.I. New correlative method of thermodynamic analysis of the inorganic compounds. March **2013**, MATEC Web of Conferences *3*, https://doi.org/10.1051/matecconf/20130301078

[3] Debye, P. Zur Theorie der spezifischen Warmen. *Annalen der Physik*. **1912**, *39*, 789-839. https://doi.org/10.1002/andp.19123441404

[4] Desnoyehs, J. E.; Morrison, J. A. The heat capacity of diamond between 12·8° and 277°K. *The Philosophical Magazine: J. Theor. Exp. Appl. Phys.* **1958**, *3*, 42-48. https://doi.org/10.1080/14786435808243223

[5] Victor, A. C. Heat Capacity of Diamond at High Temperatures. *J. Chem. Physics* **1962**, *36,* 1903-1911. https://doi.org/10.1063/1.1701288

[6] Vasil'ev, O. O.; Muratov, V. B.; Duda, T. I. The Study of Low Temperature Heat Capacity of Diamond: Calculation and Experiment. J. *Superhard Materials* **2010**, *32*, 375–382. Original Ukrainian Text: Vasil'ev, O.O.; Muratov, V.B. ; Duda, T.I. published in Sverkhtverdye Materialy, 32 (2010) 14–23. https://doi.org/10.3103/S106345761006002X

[7] Hultgren R. et al. Selected Values of the Thermodynamic Properties of the Elements, *American Society for Metals, Metals Park, Ohio* **1973**.

[8] Butland, A.T.D.; Madisson, R.J. The Specific Heat of Graphite: An Evaluation of Measurements. *J. Nucl. Mat.* **1973/74**, *49*, 45-56. https://doi.org/10.1016/0022-3115(73)90060-3

[9] Gustafson, P. An Evaluation of the Thermodynamic Properties and the P, T Phase Diagram of Carbon. *Carbon* **1986**, *24(2)*, 169. https://doi.org/10.1016/0008-6223(86)90113-2

[10] NIST-JANAF *J. Phys. Chem. Ref. Data* **1998**

[11] Savvatimskiy, A. Carbon at High Temperatures, *Springer Series, in Materials Science134* **2015**. https://doi.org/10.1007/978-3-319-21350-7_2

[12] Desai, P.D. Thermodynamic properties of Iron and Silicon. *J. Phys. Chem. Ref. Data* **1986**, *15(3),* 967- 983. https://doi.org/10.1063/1.555761

[13] Devyatykh, G.G.; Gusev, A.V.; Gibin, A.M.; Timofeev, O.V. Heat capacity of high-purity silicon. *Russian Inorganic Materials* **1997**, *33*, 1425-28.

[14] Flubacher, P.; Leadbetter A. J.; Morrison J. A. The heat capacity of pure silicon and germanium and properties of their vibrational frequency spectra, *Philosoph. Magazine* **1959**, *39*, 273-294. https://doi.org/10.1080/14786435908233340

[15] Glazov, V. M.;.Pashinkin, A. S. The thermodynamic properties (heat capacity and thermal

expansion) of single-crystal silicon. *High Temperature* **2001**, *39*, 413-419. https://doi.org/10.1023/A: 1017562709942

[16] Mills, K.C.; Courtney, L. Thermophysical Properties of Silicon. *ISIJ International* **2000**, *40*, 130-138. https://doi.org/10.2355/isijinternational.40.Suppl_S130

[17] Pearlman N.; H. Keesom, P. The Atomic Heat of Silicon below 100°K. *Phys. Rev*. **1952,** *88*, 398. https://doi.org/10.1103/PhysRev.88.398

[18] Timofeev, O.V. The Heat Capacity of High-Purity Silicon, Ph.D. Specialty 02.00.19 Nizhny Novgorod, **1999**, 199 P.; Timofeyev, O. V. Teployemkost' vysokochistogo kremniya, Kand. Diss. Spetsial'nost' 02.00.19 Nizhniy Novgorod, **1999**, 199 s.

[19] Neviak, S.O.; Sandulova, A.V. Thermodynamic characteristics of AlP. *Inorg. Materials* **1974** *10*, 146-147 (in Russian) https://doi.org/10.1134/S0020168506110021

[20] Yamagouchi, K.; Itagaki, K.; Yasawa, A. High temperature heat content measurements of the III-V (III: Al, Ga, In V: N, P, As, Sb) *J. Japan Inst. Metals*. **1989**, *53*, 764-770. https://doi.org/10.1023/A: 1020609517891

[21] Estermann, I.;Weertman, J. R. Specific Heat of Germanium between 20°K and 200°K. *J. Chem. Phys.* **1952**, *20*, 972. https://doi.org/10.1063/1.1700659

[22] Hill, R.W.; Parkinson, D.H. XXV. The specific heats of germanium and grey tin at low temperatures, *The London, Edinburgh*, and *Dublin Phil. Magazine and J. Science.* **1952**, *43:338*, 309-316. https://doi.org/10.1080/14786440308520161

[23] Sommelet, P.; Orr, R.L. High-Temperature Thermal Properties of Germanium. *J. Chem. Eng. Data* **1966**, *11*, 64-65. https://doi.org/10.1021/je60028a018

[24] Leadbetter, A. J.; Settatree, G. R. Anharmonic effects in the thermodynamic properties of solids VI. Germanium: heat capacity between 30 and 500 °C and analysis of data. *J. Phys. C: Solid State Phys*. **1969**, *2*, 1105-1112. https://doi.org/10.1088/0022-3719/2/7/301

[25] Glazov, V. M.; Pashinkin, A. S. Thermal expansion and heat capacity of GaAs and InAs, *Inorganic Materials* **2000**, *36*, 225-231. https://doi.org/10.1007/BF02757926

[26] Glazov, V. M.; Malkova, A. S.; Pavlova, L.M.; Pashinkin, A. S. The Heat Capacity of Solid Gallium Arsenide (200-1514 K). *Russ. J. Phys. Chem.* **2000**, *74*, 145*; Zh. Fiz. Khimii* **2000**, *74*, 203. https://doi.org/10.1063/1.4818273

[27] Piesbergen, U. Die durchschnittlichen Atomwärmen der $A^{III}B^{V}$ Halbleiter AlSb, GaAs, GaSb, InP, InAs, InSb und die Atomwarme des Elements Ge zwischen 12-273 K. *Naturwissenschaften* **1963**, *l8a* (№ 2) 141 -147. https://doi.org/10.1515/zna-1963-0206 Corpus ID:93466342

[28] Lichter, B.D.; Sommelet, P. Thermal Properties of $A^{III}B^{V}$ Compounds. I. High-Temperature Heat Constants and heat Fusion of InSb, GaSb, and AlSb. *Trans. Met.* **1969**, *245*, 99 -105. https://doi.org/10.2320/jinstmet1952.53.8_764

[29] Webb, F. J.; Wilks, J. The measurement of lattice specific heats at low temperatures using a heat switch, *Proc. Roy. Soc*. **1955**, *230*, 549-559. https://doi.org/10.1098/rspa.1955.0150

[30] Brönsted, J.N.; Studien zur chemischen Affinität, IX. Die allotrope Zinn Umwandlung, *Z. Phys. Chem* **1914**, *88U*, 479-489

[31] Ohmura, Y.; Specific Heat of Indium Antimonide between 6 and 100°K. J. Phys. Soc. Jpn. **1965**, *20*, 350-353. https://doi.org/10.1143/JPSJ.20.350

[32] Pässler, R.; Non-Debye heat capacity formula refined and applied to GaP, GaAs, GaSb, InP, InAs, and InSb. *AIP ADVANCES* **2013**, *3*, 082108. https://doi.org/10.1063/1.4818273

[33] Pashinkin, A.S.; Fedorov, V.A.; Mikhailova, M.S. et al., Heat capacity of solid $A^{II}Se$ and $A^{II}Te$ above 298 K. *Inorg Mater.* **2012**, *48*, 28–33. https://doi.org/10.1134/S0020168512010116

[34] Gavrichev, K.S.; Solozhenko, V.L.; Gorbunov, V.E.; Golushina, L.N.; Totrova, G.A.; Lazarev, V.B. Low-temperature heat capacity and thermodynamic properties of four boron nitride modifications. *Thermochim. Acta* **1993**, *217*, 77-89. https://doi.org/10.1016/0040-6031(93)85099-U

[35] Sirota, N.N.; Caufman, N.A. Temperature dependence of the heat capacity of boron nitride in the range 5 - 300 K. *Doklady AN SSSR* **1975**, 225, 1316-1318.

[36] Burdina, K.P. The chemical aspects of the synthesis of cubic boron nitride. Doctor Diss. Moscow, **2000**.

[37] Brito, B.G.A.; Cândido, L. Thermodynamic properties of cubic boron nitride crystal by path integral Monte Carlo simulations. *Chem. Phys. Letters* **2020**, 751, 137513. https://doi.org/10.1016/j.cplett.2020.137513

[38] Davies, G.; Evans, T. Graphitization of Diamond at Zero Pressure and at a High Pressure, *Proceedings of the Royal Society A.* **1972**, *328*, 413–27 https://doi.org/10.1098/rspa.1972.0086

[39] Bai, Q.; Wang, Zh.; Guo, Y.; Chen, J.; Shang, Y. Graphitization Behavior of Single Crystal Diamond for the Application in Nano-Metric Cutting. *Current Nanoscience* **2018**, *14*, 377-383 https://doi.org/10.2174/1573413714666180517080721

[40] Holleman, A.F.; Wiberg, E.; Wiberg, Nils (ed.) *Inorganic Chemistry* **2001**, Berlin: Academic Press/De Gruyter, ISBN 0-12-352651-5

[41] Liang, S.-M.; Schmid-Fetzer, R. Thermodynamic assessment of the Al–P system based on original experimental data, *CALPHAD* **2013**, *42*, 76–85. https://doi.org/10.1016/j.calphad.2013.07.001

[42] Vassiliev, V.P.; Gong, W.; Taldrik, A.F.; Kulinich, S.A. Method of the correlative optimization of heat capacities of isostructural compounds. *J. Alloys Comp.* **2013**, *552*, 248–254. https://doi.org/10.1051/matecconf/20130301074

[43] Dias da Silva, J. H.; Cisneros, J.I.; Guraya, M.M.; Zampieri, G. Effect of Deviation from Stoichiometry and Thermal Annealing on Amorphous Gallium Antimonide Films *Phys Rev B Condense Matter.* **1995**, *51*, No10, 6272-6279. https://doi.org/10.1103/physrevb.51.6272

[44] Avetissov, Ch.; Mozhevitina, E. N.; Khomyakov, A. V.; Avetisov, R. I.; Davydov, A. A.; Chegnov, V. P. ; Chegnova, O. I. ; Zhavoronkov, N. V. Homogeneity limits and nonstoichiometric of vapor grown ZnTe and CdTe crystals. *Cryst. Eng. Comm.* **2015**, *17*, 561. https://doi.org/10.1039/c4ce00623b

[45] Gusev, A.V. ; Gibin, A.M. ; Andryushchenko, I.A.; Gavva, V.A. ; Kozyrev E.A. Heat capacity of high-purity isotope-enriched germanium-76 in the range of 2-15K. *Solid State Physics* **2015**, *57*, 1868-1870. https://doi.org/10.1134/S1063783415090097

[46] Gibin, A.M.; Devyatykh, G.G. ; Gusev, A.V. ; Kremer, R.K.; Cardona, M.; Pohl, H.-J. Heat capacity of isotopically enriched Si-28, Si-29 and Si-30 in the temperature range 4 K T 100 K. *Solid State Communications* **2005**, *133(9),* 569-572. https://doi.org/10.1016/j.ssc.2004.12.047

[47] Yuan, C. ; Li, J. ; Lindsay, L. *et al.* Modulating the thermal conductivity in hexagonal boron nitride via controlled boron isotope concentration. *Commun Phys.* **2019**, *2*, 43. https://doi.org/10.1038/s42005-019-0145-5

[48] Pashinkin, A.S. ; Malkova, A. S.; Mikhailova, M. S. The Heat Capacity of Indium Phosphide. *Rus. J. Phys. Chem. A.* **2009**, *83,* 1051–1052. https://doi.org/10.1134/S0036024409060338

[49] Pankratz, L.B. High-temperature heat contents and entropies of gallium phosphide, indium phosphide and indium sulphide. *US Bureau of Mines Rep. Invest*. 6592; US Department of the interior: Washington. DC. **1965**. https://doi.org/10.1021/cr000039m

[50] Fornari, R.; Brinciotti, A.; Sentiri, A.; Görög, T.; Curti, M.; Zuccalli, G. Pressure of phosphorus in equilibrium with solid InP at different temperatures. *J. App. Physics* **1994**, *75,* 2406-09. https://doi.org/10.1063/1.356980

[51] *Electronic handbook: Thermodynamic Constance of Substances*. http://www.chem.msu.su/cgi-bin/tkv.pl?show=welcome.html

[52] Bundly, F.P.; Bassette, W.A. ; Weather, M.S. ; Hemlay, R.J. ; Mao, H.K. ; Goncharov, A.F. The pressure-temperature phase and transformation diagram carbon. *Carbon* **1996**, *34*, 141- 153. https://doi.org/10.1016/0008-6223(96)00170-4.

[53] Solozhenko, V.L.; Turkevich, V.; Holzapfel, W.B. Refined Phase Diagram of Boron Nitride. *J. Phys. Chem. B.* **1999**, *103*, 2903-2905. https://doi.org/10.1021/jp984682c

[54] Bigdeli, S.; Chen, Q.; Selleby, M. A New Description of Pure C in Developing the Third Generation of Calphad Databases. *J. Phase Equilib. Diffus.* **2018**, *39*, 832–840 https://doi.org/10.1007/s11669-018-0679-3)